nature cancer

Brief Communication

https://doi.org/10.1038/s43018-023-00623-x

A phase 1 trial of adoptive transfer of vaccine-primed autologous circulating T cells in ovarian cancer

Received: 18 March 2022

Accepted: 24 July 2023

Published online: 21 September 2023

Check for updates

Sara Bobisse[1,2,12], Valentina Bianchi[1,2,3,12], Janos L. Tanyi[4,12], Apostolos Sarivalasis[2], Edoardo Missiaglia[5,6], Rémy Pétremand[1,2], Fabrizio Benedetti[1,2], Drew A. Torigian[7], Raphael Genolet[1,2], David Barras[1,2], Alexandra Michel[1,2], Spyridon A. Mastroyannis[4], Emese Zsiros[4,10], Denarda Dangaj Laniti[1,2], Zoi Tsourti[8], Brian J. Stevenson[1,2,6], Christian Iseli[6,11], Bruce L. Levine[9], Daniel E. Speiser[2], David Gfeller[1,2,6], Michal Bassani-Sternberg[1,2], Daniel J. Powell Jr[9], Carl H. June[9], Urania Dafni[8], Lana E. Kandalaft[1,2,3,13], Alexandre Harari[1,2,13] & George Coukos[1,2,13] ✉

We have previously shown that vaccination with tumor-pulsed dendritic cells amplifies neoantigen recognition in ovarian cancer. Here, in a phase 1 clinical study (NCT01312376/UPCC26810) including 19 patients, we show that such responses are further reinvigorated by subsequent adoptive transfer of vaccine-primed, ex vivo-expanded autologous peripheral blood T cells. The treatment is safe, and epitope spreading with novel neopeptide reactivities was observed after cell infusion in patients who experienced clinical benefit, suggesting reinvigoration of tumor-sculpting immunity.

Although ovarian tumors are, in principle, immunoreactive[1], most patients with ovarian cancer (OC) do not benefit from immune checkpoint immunotherapy[2] and thus require alternative approaches. We previously reported a pilot study (NCT01132014/UPCC19809) in which patients with recurrent OC were vaccinated with autologous monocyte-derived dendritic cells (DCs) loaded with oxidized autologous whole-tumor lysate (termed OCDC), combined with intravenous infusion of bevacizumab and low-dose cyclophosphamide[3]. Vaccination amplified preexisting neoantigen-specific responses with new high-avidity T cell clonotypes, elicited new T cell reactivities against previously unrecognized tumor neopeptides and produced clinical benefit[3].

Inspired by these findings, we designed a follow-on study (NCT01312376/UPCC26810) in which patients were offered further treatment with adoptive cell transfer (ACT) of vaccine-primed autologous peripheral blood T cells, followed by OCDC vaccine support (generated in UPCC19809), and bevacizumab to promote T cell tumor homing[2] (Fig. 1a,b). We hypothesized that this treatment would allow reprogramming of the immune system and reinvigoration of antitumor immunity with further vaccination. We enrolled 19 patients (Extended

[1]Ludwig Institute for Cancer Research, Lausanne Branch, University of Lausanne, Lausanne, Switzerland. [2]Center for Cell Immunotherapy, Department of Oncology, University Hospital of Lausanne (CHUV), Lausanne, Switzerland. [3]Center for Experimental Therapeutics, Department of Oncology, University Hospital of Lausanne (CHUV), Lausanne, Switzerland. [4]Division of Gynecologic Oncology, Department of Obstetrics and Gynecology, Hospital of the University of Pennsylvania, Philadelphia, PA, USA. [5]Institute of Pathology, University Hospital of Lausanne (CHUV), Lausanne, Switzerland. [6]SIB Swiss Institute of Bioinformatics, Lausanne, Switzerland. [7]Department of Radiology, Hospital of the University of Pennsylvania, Philadelphia, PA, USA. [8]Laboratory of Biostatistics, School of Health Sciences, National and Kapodistrian University of Athens, Athens, Greece. [9]Center for Cellular Immunotherapies, University of Pennsylvania, Philadelphia, PA, USA. [10]Present address: Department of Gynecologic Oncology, Roswell Park Comprehensive Cancer Center, Buffalo, NY, USA. [11]Present address: Bioinformatics Competence Center, École Polytechnique Fédérale de Lausanne, Lausanne, Switzerland. [12]These authors contributed equally: Sara Bobisse, Valentina Bianchi, Janos L. Tanyi. [13]These authors jointly supervised this work: Lana E. Kandalaft, Alexandre Harari, George Coukos ✉e-mail: george.coukos@chuv.ch

https://doi.org/10.1038/s43018-023-00623-x

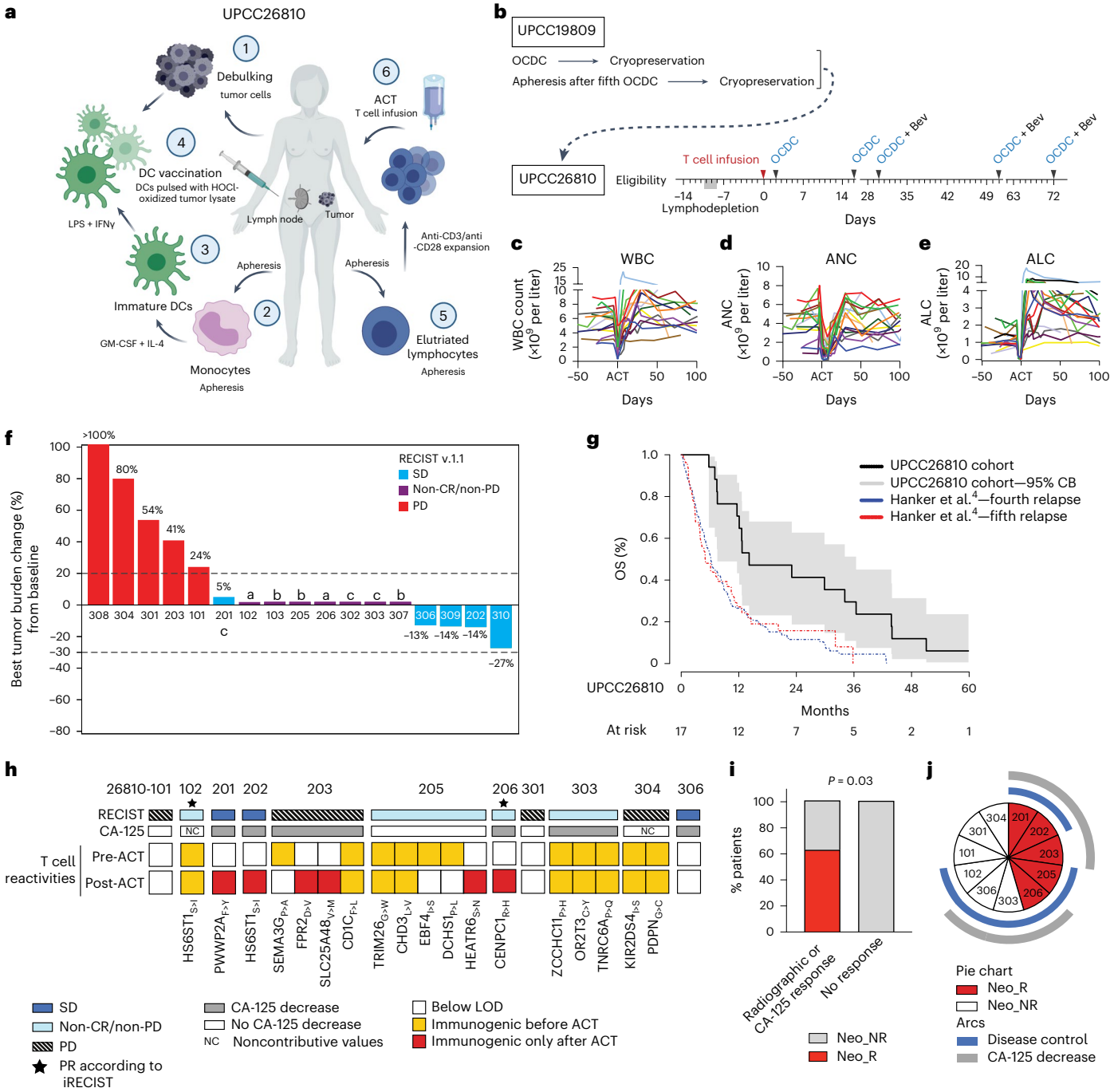

Fig. 1 | Adoptive transfer of ex vivo-expanded T cells is followed by rapid hematologic reconstitution and clinical benefit. a,**b**, Scheme (**a**) and timeline (**b**) of the therapy. Created with BioRender.com. LPS, lipopolysaccharide; GM-CSF, granulocyte–macrophage colony-stimulating factor; Bev, bevacizumab. **c**–**e**, Longitudinal absolute counts of white blood cells (WBC; **c**), neutrophils (ANC; **d**) and lymphocytes (ALC; **e**); $n = 17$ patients. Different colored lines represent individual patients. **f**, Waterfall plot detailing the best tumor burden change from baseline for each patient, according to RECIST v.1.1. Non-CR/non-PD, patients with nonmeasurable disease (according to RECIST) at all tumor assessments including baseline. Dashed lines represent the thresholds for partial response (PR), stable disease (SD) and progressive disease (PD) of target lesions according to RECIST 1.1. [a]Partial response according to iRECIST. [b]SD according to iRECIST. [c]PD according to iRECIST. **g**, Median OS estimated using the Kaplan–Meier method for the UPCC26810 study and after the fourth and fifth relapse in ref. 4; number of patients at risk for the Hanker et al.[4] curves (fourth and fifth relapse) is not available. CB, confidence band. **h**, Cumulative landscape of clinical outcomes and neopeptide-specific CD8$^+$ T cell responses before and after ACT. PR, partial response; LOD, limit of detection. **i**, Proportion of patients with neopeptide spreading (that is, newly induced neopeptide reactivities (Neo_R)) versus those with only preexisting/undetected reactivities (Neo_NR), stratified by clinical outcome (radiographic or CA-125 response, $n = 8$; no response, $n = 3$). A one-tailed chi-square test was performed for contingency analysis. **j**, Cumulative analysis of 11 patients. The pie chart reports patients color-coded for neopeptide reactivities (Neo_R versus Neo_NR), and the arcs show their clinical outcome (radiographic regression and CA-125 decrease).

https://doi.org/10.1038/s43018-023-00623-x

Data Table 1). Peripheral blood T cells, collected after five vaccinations during the UPCC19809 study, were expanded with anti-CD3/anti-CD28 beads plus interleukin-2 (IL-2; Extended Data Fig. 1a) and administered ($8.9–27 \times 10^9$ cells; Extended Data Table 2) on day 0 following lymphodepletion by intravenous infusion of cyclophosphamide (300 mg m^{-2}) and fludarabine (30 mg m^{-2}) on days −6 to −4. One patient withdrew from the study before receiving any treatment, and a second patient withdrew before receiving T cell infusion. All remaining patients received, in an outpatient setting, ACT and pegfilgrastim on day 0; OCDC vaccine ($5–10 \times 10^6$ DCs) on days 2, 16 and 30 after ACT and every 3 weeks thereafter (median 5 doses, range 1–13 doses); and intravenous infusion of bevacizumab until disease progression.

Among the 19 patients enrolled, 18 received lymphodepletion and 17 (89.5%) completed the entire combination treatment, rendering the overall treatment feasible. Severe adverse events were mainly hematologic (Extended Data Table 3), with no grade 5 severe adverse events, immune-related or T cell-related severe adverse events, or clinical viral reactivation. Four patients required hospitalization; one patient had febrile neutropenia and three patients had grade 3 dehydration, with one case associated with seizures but without brain imaging findings. Grade 4 proteinuria, related to bevacizumab, was the only treatment-limiting toxicity (TLT; 6% of patients), rendering the study treatment safe.

White blood cell nadir ($2.22 \pm 1.4 \times 10^9$ cells per liter, range $0.3–3.9 \times 10^9$ cells per liter) was reached on days 0–4 (Fig. 1c), and absolute neutrophil nadir ($0.69 \pm 0.85 \times 10^9$ cells per liter, range $0.11–2.97 \times 10^9$ cells per liter) was reached on days 2–10 (Fig. 1d). Absolute lymphocyte nadir ($0.04 \pm 0.03 \times 10^9$ cells per liter, range $0–0.1 \times 10^9$ cells per liter) was reached on days −2 to 0 (Fig. 1e). Lymphoid reconstitution following ACT was rapid, with the absolute lymphocyte count persisting above the baseline for several weeks in most patients (Fig. 1e). The highest absolute lymphocyte count ($4.29 \pm 3.37 \times 10^9$ cells per liter, range $1.01–15.42 \times 10^9$ cells per liter) was reached on day 24 (range, days 7–85) after ACT and did not correlate with the absolute lymphocyte nadir after lymphodepletion or the ex vivo T cell proliferation (Extended Data Fig. 1b,c). Remarkably, we observed a significantly increased frequency of circulating $CD8^+$ T cells and a significantly decreased frequency of circulating monocytes, B cells and plasmacytoid DCs after ACT (Extended Data Fig. 2a,b).

In these heavily pretreated, platinum-resistant patients, ACT followed by vaccine and bevacizumab resulted in disease control (according to Response Evaluation Criteria in Solid Tumors (RECIST) v.1.1) at 3 months in 12 of 17 patients (70.5%; Fig. 1f). Among these, seven patients had nonmeasurable disease according to RECIST, two of whom had a partial response according to the immune RECIST (iRECIST) criteria and three had dissociated radiographic responses, with regression of some lesions, and a decrease in the serum carbohydrate antigen 125 (CA-125) level by 12 weeks. The median overall survival (OS) was 14.2 months (range 5.8–76.9 months, 95% confidence interval (CI) 7.6–36.5 months), exceeding the historical median OS of patients with advanced OC beyond third-line chemotherapy, reported as 6.2 months (95% CI 5.1–7.7 months) for fourth line and 5.0 months (95% CI 3.8–10.4 months) for fifth line[4] (Fig. 1g).

To capture the immune effects of therapy, we interrogated $CD8^+$ T cell responses to neopeptides from nonsynonymous somatic tumor mutations[5], comparing seven patients who had any evidence of a radiographic response (that is, either partial response according to iRECIST ($n = 2$) or stable disease or nonmeasurable disease according to RECIST with a dissociated radiographic response plus a CA-125 response ($n = 5$)) to four patients who had no radiographic response (progression of all tumor lesions). ACT restored preexisting immunity to neopeptides (Fig. 1h, Supplementary Figs. 1–5 and Extended Data Table 4); in five patients in whom neopeptide-reactive $CD8^+$ T cells were found before ACT, we detected responses to most neopeptides after ACT. Furthermore, therapy elicited new responses, expanding the recognition of neopeptides after ACT in three additional patients, with six newly identified neopeptides (Fig. 1h, Supplementary Figs. 1–5 and Extended Data Tables 4 and 5). Most of the circulating neopeptide-specific T cells after ACT were polyfunctional (Extended Data Fig. 3a,b). Importantly, we observed an association between the detection of new neopeptide responses after ACT and any radiographic response (global or dissociated) or serum CA-125 response, the latter being a highly sensitive biomarker of mixed responses[6–8] (Fig. 1i). Moreover, three patients with no neopeptide spreading after ACT had neither a radiographic nor a CA-125 response (Fig. 1i,j).

The above clinical results are consistent with the known molecular intrapatient heterogeneity of OC. To learn more, we evaluated circulating tumor DNA (ctDNA) levels for 22 identified private mutations[9]. In patient 206 with concordant partial response of all lesions (iRECIST; Fig. 2a), we noted transient elevation of ctDNA levels for the cognate neopeptide after ACT (Fig. 2b). This coincided with a decrease in the serum CA-125 level (Fig. 2c), suggesting that the release of ctDNA may herald immune attack, as previously described for ACT of tumor-infiltrating lymphocytes[10]. Cumulatively, we detected ctDNA before ACT for only a small fraction of single-nucleotide variants (SNVs) in the assessed patients, with no difference between immunogenic and nonimmunogenic mutations (Extended Data Fig. 4a). However, we observed an increase in the number of detected ctDNA fragments after ACT, specifically for immunogenic mutations (Fig. 2d–g and Extended Data Fig. 4a,b). Further investigation is required to test whether ctDNA dynamics reflect a divergent evolution of clonal tumor populations under therapeutic pressure and to examine their use in monitoring tumor response to adoptive immunotherapy.

The management of late-line recurrent OC remains challenging[2,11]. Here, we show reinvigoration of antitumor immunity by ACT of vaccine-primed peripheral blood T cells with additional OCDC vaccination. Although this therapy was not sufficiently potent to eradicate tumors, it produced clinical benefit. Moreover, important lessons can

Fig. 2 | Elevated ctDNA levels after ACT are specifically associated with immunogenic mutations. a, Computed tomography scans of patient 206 showing regression of tumor deposits (yellow arrows) in a periaortic lymph node (lesion A) and an obturator lymph node (lesion B). **b**, Allele frequency (% AF; that is, percentage of mutated reads over the total reads) in ctDNA evaluated at different time points for the SNV *CENPCI*^{R738H} in patient 206. EOS, end of study. **c**, Serum CA-125 levels in patient 206 during the UPCC26810 study. Day 30 is identified with a gray arrow. **d**, Representative examples of T cell response (by IFNγ ELISpot assay; top) and ctDNA analyses (bottom). We show the allele frequency evaluated before and after ACT together with the cognate neopeptide-specific T cell responses measured before and after ACT in patient 205. Allele frequency and T cell responses are shown for the $CHD3_{L>V}$, $DCHS1_{P>L}$, $HEATR6_{S>N}$ and $TRIM26_{G>W}$ neopeptides and are color-coded based on their immunogenicity. Allele frequency is also provided for *BIRC6* and *TTC24* (control nonimmunogenic SNVs) and *OBP2A* (reference SNP). The variant allele frequency (VAF) in tumors at the time of collection for vaccine preparation is reported at the bottom of each SNV. NA, not assessed. **e**, Assessment, in pre- and post-ACT samples, of ctDNA levels for all 22 variants successfully analyzed (left, already detected before ACT ($n = 10$); right, not detected before ACT ($n = 12$)). ctDNA levels are expressed as *z* scores. Variants are separated and color-coded based on the immunogenicity of cognate SNVs. **f**, Overview of the pre- and/or post-ACT immunogenicity of all 13 immunogenic SNVs concomitant with the detection of cognate ctDNA. White boxes: negative; yellow and red boxes: T cell responses detected already pre-ACT or only post-ACT respectively; crosses: concomitant detection of ctDNA. **g**, Immunogenicity of the different SNVs was considered at the time of the analysis (that is, neopeptides detected only after ACT were considered nonimmunogenic before ACT), as per **f**. Histograms show the cumulative analyses of the fraction of ctDNA variants ($n = 22$) detected, based on the immunogenicity of cognate SNVs, before ACT (left) and after ACT (right). Data were assessed using a one-sided chi-square test.

https://doi.org/10.1038/s43018-023-00623-x

be learned from the medium-intensity lymphodepletion and the use of CD28-costimulated cells, which enabled rapid neutrophil recovery and lymphoid reconstitution, respectively. Although other possible neopeptide sources were not investigated and tumor targeting by neopeptide-specific CD8$^+$ T cells could not be ruled out, monitoring for T cell responses against neopeptides derived from nonsynonymous SNVs is sufficient to show that the treatment restores prior antitumor immunity and induces neopeptide spreading, which correlates with tumor response. The heterogeneity of OC represents an important therapeutic challenge. Tumor lysate was originally prepared from a single lesion in these patients with widely metastatic disease. Therefore, the elicited responses to tumor-specific antigens may have been limited and not representative of the tumor antigenome across lesions. ACT of tumor-infiltrating lymphocytes faces similar challenges[12], suggesting that ACT strategies for OC must include a broad tumor antigen representation.

Methods

Study design

This single-center phase 1 study (NCT01312376/UPCC26810) of adoptive transfer of vaccine-primed, CD3/CD28-costimulated T cells after lymphodepletion followed by OCDC vaccination and bevacizumab

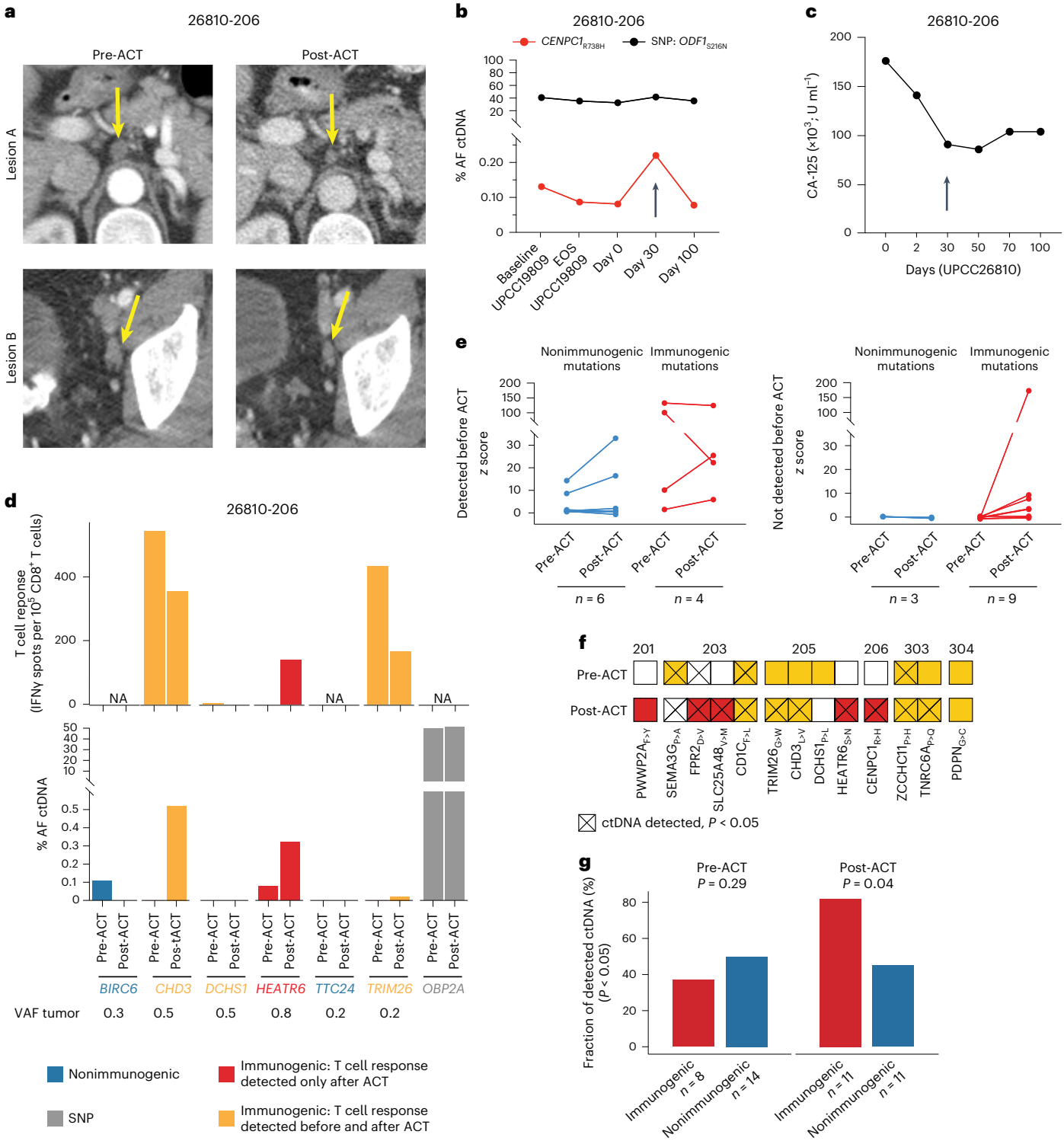

consolidation was conducted in the gynecologic oncology service at the University of Pennsylvania (UPenn) Medical Center, under an investigational new drug application accepted by the US Food and Drug Administration. The clinical protocol was approved by the local institutional review board and independent medical safety monitors at UPenn. The study was started in March 2011 and terminated in January 2019, with patient enrollment from March 2011 through February 2014. T cells were manufactured at the Clinical Cell and Vaccine Production Facility of UPenn. The primary objective was to determine the feasibility and safety of ACT of vaccine-primed, ex vivo CD3/CD28-costimulated autologous peripheral blood T cells, in combination with lymphodepletion and an immunomodulation regimen with bevacizumab followed by autologous vaccination. Feasibility was assessed based on the number of patients who successfully received the combination treatment. Safety was assessed based on the occurrence of TLT. If TLT was observed in >33% of patients, the therapy was considered excessively toxic (that is, >33% of patients with toxicity is not acceptable). Additional objectives included the determination of the patients' immune function, antitumor immune response, tumor burden, immune-related progression-free survival, OS and time to progression. No statistical methods were used to predetermine sample sizes, but our sample sizes are similar to those reported in previous publications[3]. Data collection and analysis were not performed blind to the conditions of the experiments. In this pilot study, up to 12 participants were planned to enter the study in a nonrandomized dose-escalation scheme with three doses: $10–15 \times 10^9$, $20–30 \times 10^9$ and $40–50 \times 10^9$ T cells. Three patients (101–103) received the entry dose (specifically, $13.6–15 \times 10^9$ T cells; Extended Data Table 2), followed by three additional patients (201–203) who received the second dose ($10.9–27.3 \times 10^9$ T cells). Because patient 203 received less than the minimum of 20 billion cells, we extended cohort 2 to collect additional safety data. We enrolled three patients but treated two additional patients, who received 8.9×10^9 and 18×10^9 cells. In five of the first eight patients, we did not obtain, at the manufacturing stage, a cell number compatible with the minimum dose for cohort 3 (40×10^9 cells), and none of these patients had a safety signal with dose 1 or 2; thus, we decided to modify the design and proceed with an extension cohort, using a dose of 20×10^9 T cells, which was shown to be safe. We treated nine additional patients with the fixed dose of 20×10^9 cells. A total of 18 patients received lymphodepletion, and 17 patients received T cells followed by vaccine and bevacizumab. One patient voluntarily withdrew from the study before receiving any treatment; another patient (204) developed acute myocardial infarction after lymphodepletion, which was deemed unrelated to chemotherapy, and was not treated with T cells.

Regarding manufacturing feasibility, we manufactured T cells for all 19 patients. The fixed dose of 20×10^9 T cells was met in all nine patients who were treated in the extension cohort. Interestingly, we were able to manufacture a sufficient number of cells for the original dose of $>40 \times 10^9$ cells for all patients in the extension cohort. Overall, these results show the feasibility of manufacturing and administering vaccine-primed, ex vivo CD3/CD28-costimulated autologous peripheral blood T cells at a dose of 20×10^9 cells, with prior lymphodepletion with cyclophosphamide and fludarabine followed by autologous vaccination and bevacizumab.

Study population

All participants signed the informed consent form. Eligible patients had a diagnosis of epithelial ovarian, fallopian tube or primary peritoneal adenocarcinoma and exhibited persistent or progressive disease (according to RECIST) after intervening therapy or after at least five vaccine administrations in the prior protocol (NCT01132014/UPCC19809, a clinical study administering OCDC vaccine in combination with intravenous infusion of low-dose cyclophosphamide and bevacizumab). Patients were eligible for UPCC26810 provided we had collected peripheral blood T cells through apheresis after vaccination in the UPCC19809 study and they had at least two more vaccine doses available. All patients were aged ≥18 years, had an Eastern Cooperative Oncology Group performance status of 0 or 1 and had a life expectancy of >4 months. All patients had normal organ and bone marrow function, defined by the following parameters: absolute neutrophil count >1,000 cells per microliter; platelet count >100,000 cells per microliter; hematocrit >30%; aspartate transaminase and alanine transaminase levels <2.5 times the institutional upper limits of normal; bilirubin level <2.0 mg dl^{-1}, unless secondary to bile duct blockage by a tumor; and creatinine level <1.8 mg dl^{-1}. Noneligibility criteria included history or symptoms suggestive of partial or complete bowel obstruction, >2 weeks of corticosteroid treatment or other immunosuppressive treatment, acute infections and acquired clinically relevant concomitant conditions contraindicating the study therapy or interfering with the interpretation of results. The presence of serum anti-Yo antibodies on screening, irrespective of clinical relevance, was an exclusion criterion.

Intervention

All enrolled patients had undergone (in the preceding protocol, NCT01132014/UPCC19809) leukapheresis of 15 L of blood after five vaccinations, to isolate vaccine-primed peripheral blood lymphocytes. At 32–375 days following the completion of UPCC19809, patients enrolled in the current protocol (NCT01312376/UPCC26810) received adoptive transfer of vaccine-primed T cells expanded ex vivo with CD3/CD28 costimulation, followed by OCDC maintenance in combination with bevacizumab. The termination criteria were inadequate autologous T cell expansion levels and the occurrence of TLT from any of the investigational products. TLT was defined as any of the following events: persistent grade 4 hematologic toxicity, grade 3/4 transfusion reactions, graft versus host disease-like manifestations, or autoimmune manifestations other than central nervous system events or any life-threatening events. Excessive toxicity was defined as the occurrence of TLT in more than one-third of patients. Patients who had radiographic disease progression (according to RECIST v.1.1) on computed tomography imaging exited the study and were followed for survival. Elevation of serum CA-125 levels was monitored until radiologic confirmation of progressive disease but was not taken into consideration for study decisions.

Data collection and analysis

Demographic and disease characteristics of all eligible patients, including age, initial disease stage and histology, and number of prior treatment lines, were collected for analysis. The number of OCDC administrations before ACT and the comedications within the NCT01132014/UPCC19809 study, as well as the number of post-ACT OCDC administrations, were recorded. Data on the best radiologic response according to iRECIST, longitudinal CA-125 values[6] before and after ACT, and time to death from enrollment into NCT01312376/UPCC26810 were collected.

Cell product preparation

Peripheral blood lymphocytes were isolated by leukapheresis of 15 L of blood in the UPCC19809 study. Monocytes were depleted by counterflow centrifugal elutriation (Elutra cell separation system, Terumo BCT). Enriched fresh T cells were cryopreserved during the UPCC19809 study. Following enrollment, the frozen T cells were thawed and expanded ex vivo at the Clinical Cell and Vaccine Production Facility at UPenn, using anti-CD3/anti-CD28 beads plus IL-2 for 11 days according to previously reported protocols[13,14] (Extended Data Fig. 1a). Briefly, cells were seeded into gas-permeable flasks (Lifecell, Baxter). Cells were grown in X-VIVO medium supplemented with 5% commercial pooled human AB serum. Dynal microbeads coated with anti-CD3/anti-CD28 antibodies were added to the cells at a 3:1 (beads to cell) ratio. The cells were counted, and fresh medium was added throughout the expansion to maintain an appropriate cell density.

For final product preparation, cells were expanded ex vivo for up to 11 days and then collected on the designated infusion date. Culture samples were obtained for flow cytometry and endotoxin, bacterial and fungal testing to determine whether the final product release criteria were met. On collection day, the microbeads were removed using a Baxter Fenwal Maxsep magnetic cell separator, washed and concentrated using the Baxter Fenwal Harvester system, and resuspended in 100–300 ml of a 1:1 dilution of PlasmaLyte A/5% dextrose, 0.45% NaCl containing 0.5–1% human serum albumin. For reinfusion clearance of the expanded T cell product, a minimum cell viability percentage of ≥80% for fresh products or ≥70% for cryopreserved products was required. The CD3 concentration on day 7 or later had to be >80% by fluorescence-activated cell sorting (FACS), with <100 residual microbeads per 3×10^6 cells. Cell cultures had to be negative for bacteria and fungi at 96–48 h before collection, with negative Gram stain of a sample of the precollection cells and <1 endotoxin unit per milliliter at 24–48 h before collection. Median expansion of T cells was 38-fold (range 8- to 82-fold), reaching a median of 43×10^9 (range $10–64.2 \times 10^9$) collected T cells (Extended Data Table 2).

Cell product administration

In preparation for ACT, patients received, in an outpatient setting, intravenous infusion of high-dose cyclophosphamide at 300 mg m^{-2} per day for 3 days and intravenous infusion of fludarabine at 30 mg m^{-2} per day for 3 days to achieve lymphodepletion. On day 0, patients were infused (as outpatients) with the available T cell product ($8.9–27.3 \times 10^9$ T cells) resuspended in a total volume of 100–300 ml, intravenously administered over 20–30 min without a leukocyte filter after premedication with acetaminophen and diphenhydramine. The T cell infusion was followed by vaccine maintenance with OCDC within 2 days, as a way to support and expand the tumor-reactive T cells in vivo after the transfer.

OCDC preparation

Details on the preparation of autologous DCs and the OCDC vaccine product are provided in the article reporting the preceding study (NCT01132014/UPCC19809)[3]. Briefly, peripheral blood mononuclear cells (PBMCs) were isolated by leukapheresis of 10 L of blood. Adherent monocytes were cultured for 4 days with IL-4 and granulocyte–macrophage colony-stimulating factor to generate immature DCs, which were pulsed with tumor lysate and then matured with lipopolysaccharide and recombinant human interferon-γ (IFNγ). OCDC aliquots were viably cryopreserved in liquid nitrogen at $5–10 \times 10^6$ cells per vial.

Immune profiling of PBMCs through density-based automated gating and clustering

Thawed PBMC samples collected from six representative patients before ACT and 30 days after T cell transfer were stained to characterize peripheral immune cell populations, with particular emphasis on lymphocytes. The immune profiling antibody panel (BD Biosciences unless otherwise stated) included CD3-APC (Beckman Coulter), CD4-PE Cy7, CD8-Pacific Blue, CD14-APC H7, CD16-FITC, CD56-PE (Beckman Coulter), CD11c-AF700, CD19-BV711, CD123-PerCP Cy5.5 (eBioscience), HLA-DR-ECD and Indo-violet viability dye (BioLegend). PBMC samples from two healthy donors were analyzed as controls. PBMC collection followed the legal Swiss guidelines under project P_123, with informed consent from the donors and ethics approval from the Canton of Vaud (Lausanne). Flow cytometry was performed using an LSR Fortessa flow cytometer (BD Biosciences). An automatic gating strategy was applied to compensate and 'logicle' transform the flow cytometry files. One- and two-dimensional gating methods, such as 'mindensity' and 'singletGate' from the R package, were used to clean data of dead cells, debris and doublets. For population identification, 'FlowSOM' clustering was used to generate 40 clusters, which were further manually reduced to 10 macroclusters based on shared cell markers. Initially, we identified clusters of the main PBMC lymphoid and myeloid lineages based on lineage marker expression. Subsequently, to obtain sufficiently high resolution for further analysis and to calculate frequencies within individual cell populations, clusters were manually merged into cell subsets according to consensual marker-expression patterns. Data were visualized and statistically analyzed in R package for patient stratification.

Identification of nonsynonymous tumor mutations and peptide prediction

Genomic DNA from 11 cryopreserved tumor tissues and matched PBMCs was isolated using a DNeasy kit (Qiagen) and subjected to whole-exome capture and paired-end sequencing on the HiSeq2500 Illumina platform. Prediction of nonsynonymous somatic tumor mutations was exclusively performed at the baseline of the UPCC19809 study, given that this represents the unique source of tumor material from these patients. Somatic variants for all 11 patients were called as previously described[5]. Variations present in the tumor samples and absent from the corresponding blood samples were assumed to be somatic.

Prediction of neoepitope binding to class I human leukocyte antigen (HLA) alleles, for all candidate peptides incorporating somatic nonsynonymous mutations, was performed using the NetMHC v.3.4 algorithm as previously described[5]. Candidate neoepitope peptides and their wild-type native predicted peptides were synthesized (at >90% high-performance liquid chromatography purity) at the Protein and Peptide Chemistry Facility, University of Lausanne. High-resolution HLA typing at the A, B and C loci was performed at the Immunogenetics Laboratory, Department of Pathology and Laboratory Medicine, Children's Hospital of Philadelphia, using a next-generation sequencing protocol.

In vitro identification and characterization of neoepitope-specific T cells

Immune recognition of tumor neopeptides was assessed in blood collected at baseline (entry in the present study) and after ACT from 11 patients in whom nonsynonymous tumor mutations had been identified. In all patients, $CD8^+$ T cells were interrogated after a first round of in vitro stimulation (IVS) with a peptide or peptide pools to assess the presence or absence of neopeptide reactivity, as previously described[5], with minor modifications. Briefly, $CD8^+$ T cells (10^6 cells per milliliter) were negatively selected (Miltenyi Biotec) from cryopreserved PBMCs and cocultured with irradiated, $CD8^+$ and $CD4^+$ T cell-depleted autologous PBMCs (at a 1:1 ratio) and peptides (1 μg ml^{-1}, single peptide or pools of ≤50 peptides) in 96-well U-bottom plates. IFNγ ELISpot assay was performed on day 12 as previously described[5], using precoated ELISpot plates (Mabtech), and spot-forming units were counted using a Bioreader-6000-E automated counter (BioSys). In all IFNγ ELISpot assays, we considered as positive conditions those with an average number of spots higher than the counts of the negative control (no antigen) + 3 s.d. of the negative control. Positive responses were then deconvoluted (using leftover cells from the same IVS) to map single neopeptides. To validate immunogenic peptides, replicate independent experiments were performed after one round of IVS with peptide pools and/or single immunogenic peptides. Alternatively, when samples were not available, a second round of stimulation (IVS2) was performed to further validate T cell responses. Intracellular cytokine staining (ICS) was performed on purified neopeptide-specific T cells. First, cells were FACS-sorted based on 4-1BB (tumor necrosis factor ligand superfamily member 9) upregulation upon overnight coculture with peptide-pulsed (1 μM) autologous $CD4^+$ blasts at a 1:1 ratio. Cells stained with the Aqua viability marker (Thermo Fisher Scientific), anti-CD3 (BioLegend), anti-CD8 (BD Biosciences) and anti-human 4-1BB (Miltenyi Biotec) were sorted on a BD FACS Melody cell sorter (BD Biosciences). Purified cells were expanded, in the presence of irradiated

feeder cells from two donors at a 1:1 ratio, in complete medium supplemented with 1 µg ml^{-1} phytohemagglutinin and 150 IU ml^{-1} recombinant human IL-2. For ICS, expanded CD8$^+$ T cells were rechallenged with peptide-pulsed autologous CD4$^+$ blasts at a 1:1 ratio, in the presence of the protein transport inhibitor GolgiPlug (BD Biosciences) and CD107a-FITC (BD Pharmingen). After 16–18 h, cells were collected and stained extracellularly with CD3-APC Fire 750 (BioLegend) and CD8-PB (BD Biosciences) and then permeabilized (BD Biosciences) and stained intracellularly with IL-2-PE (BD Biosciences), TNFα-PE Cy7 (BD Biosciences), IFNγ-APC (BD Biosciences) and LIVE/DEAD Aqua viability dye (Thermo Fisher Scientific). Flow cytometry was performed using an LSR Fortessa cell analyzer (BD Biosciences), and data were analyzed using FlowJo v.10.8.1 (TreeStar) and SPICE v.6.1. Background reactivity was determined using unstimulated cells.

ctDNA mutational profiling

The MagMAX cell-free DNA (cfDNA) isolation kit (cat. no. A29319, Thermo Fisher Scientific) was used to isolate cfDNA from 2-ml serum samples. Serum samples were lysed with proteinase K (20 mg ml^{-1}, Thermo Fisher Scientific) for 20 min at 60 °C. cfDNA was isolated according to the user guide of the MagMAX cfDNA isolation kit. A set of 18 cfDNA samples were verified for genomic contamination and specific cfDNA fragment size on the Fragment Analyzer system with the High Sensitivity (HS) Genomic DNA kit (protocol DNF-488-33, Agilent). The concentration of the purified cfDNA was measured using the Qubit double-stranded DNA HS assay kit on a Qubit fluorometer. cfDNA samples <1.2 ng µl^{-1} were concentrated using the Microcon DNA Fast Flow centrifugal filter unit with an Ultracel membrane (MRCF0R100, Merck Millipore; Extended Data Table 6). An amplicon-based DNA library was prepared using a customized primer panel (custom Ion AmpliSeq panel, Ion Torrent, Thermo Fisher Scientific; Extended Data Table 6) targeting regions with private mutations. In particular, we included all 18 immunogenic SNVs; in addition, we included 16 control SNVs (that is, 2 per patient) chosen randomly from nonimmunogenic peptides and 16 single-nucleotide polymorphisms (SNPs; that is, 2 per patient) also chosen randomly as controls. Primers were designed using Ion AmpliSeq Designer v.5.63, starting from the list of variants to be monitored in serum. Libraries were manually prepared using the Ion AmpliSeq Library kit v.2.0 (Thermo Fisher Scientific) according to the manufacturer's instructions. In 14 samples, emulsion was performed using the Ion Personal Genome Machine (PGM) Hi-Q OT2 kit and sequencing was performed using an Ion 318 Chip v.2 BC with the Ion PGM Hi-Q sequencing kit on the Ion PGM System for 500 cycles (Thermo Fisher Scientific). For the remaining samples, emulsion was performed using the Ion 540 Kit-Chef with an Ion Chef instrument and sequencing was performed using an Ion 540 Chip kit on the Ion S5 System for 500 cycles in batches of 24 samples. FASTQ files were generated using Torrent suite software v.5.2.2. Bioinformatic analysis was performed using proprietary and open-source software. Briefly, reads were aligned to the human genome (Genome Analysis Toolkit (GATK) repository, build 37 decoy) with Novoalign v.3.02.07 (default setting). The median coverage was 5,900× (range 2,587–11,187×) for the PGM set and 32,411× (range 18,701–54,266×) for the S5 set of samples. SNV calling was performed, using bam-readcount v.0.8.0, only on the specific sites of interest and considering reads with a minimum mapping quality of 10. All retained alterations were confirmed by visual inspection with IGV software v.2.3. A total of 37 regions were successfully amplified: 13 of 18 regions including private immunogenic mutations, 9 of 16 regions including private nonimmunogenic mutations and 15 of 16 regions including SNPs (Extended Data Table 6). Notably, the 22 mutations included in the ctDNA analysis were validated using the GATK HaplotypeCaller, MuTect v.1 and VarScan v.2 algorithms. Moreover, the two groups of somatic mutations (immunogenic versus nonimmunogenic) showed comparable allele frequencies (Extended Data Table 6) in the original tumor samples. We estimated the background distribution of allele frequencies through the mean and s.d. to compute the *z* score, using normal approximation for candidate mutations[15]. The ~99.7% prediction interval was standardly defined as a range of 3 s.d. and corrected for aberrant whiskers below zero. *P* values were defined as the tail probability and corrected for multiple testing using Bonferroni correction. These steps were performed using the 'stats' library in R v.4.0.3.

Statistical analyses

OS was calculated for the patients receiving ACT (that is, 17 of the 19 total enrolled patients), with the start date being the UPCC26810 enrollment date. The Kaplan–Meier method was used to depict survival curves and estimate the median OS. Relevant historical data[4] were extracted from published Kaplan–Meier plots by using WebPlotDigitizer (https://apps.automeris.io/wpd). A waterfall plot was also created to present the best percentage change in total tumor burden (sum of diameters (in millimeters) of the target and new lesions) according to RECIST compared to the baseline tumor assessment before ACT. A >10% decrease in the serum CA-125 level was considered clinically relevant.

For all experimental analyses, the statistical tests used and their specifications are described in the figure legends. Differences between averages of variables were compared using a one-tailed *t* test for variables with a normal distribution (all laboratory analyses), in which data assumed to be normal were not formally tested. Nonparametric tests were used only for the comparison of allele frequencies in cfDNA for immunogenic and nonimmunogenic mutations before and after ACT. Statistical analyses were performed using GraphPad Prism v.9 and SAS v.9.4.

Reporting summary

Further information on research design is available in the Nature Portfolio Reporting Summary linked to this article.

Data availability

Exome data are available from the European Genome-phenome Archive (EGA) database under accession code EGAS00001002803. The access control to sequence data implemented at the EGA confers patient confidentiality. Cell-free DNA data are available from the European Nucleotide Archive under accession code PRJEB64132 (secondary accession no. ERP149263). The full study protocol is publicly available and provided as Supplementary Protocol. Further information on research design is also available in the Nature Portfolio Reporting Summary linked to this article. Source data are provided with this paper.

References

1. Zhang, L. et al. Intratumoral T cells, recurrence, and survival in epithelial ovarian cancer. *N. Engl. J. Med.* **348**, 203–213 (2003).
2. Kandalaft, L. E., Dangaj Laniti, D. & Coukos, G. Immunobiology of high-grade serous ovarian cancer: lessons for clinical translation. *Nat. Rev. Cancer* **22**, 640–656 (2022).
3. Tanyi, J. L. et al. Personalized cancer vaccine effectively mobilizes antitumor T cell immunity in ovarian cancer. *Sci. Transl. Med.* **10**, eaao5931 (2018).
4. Hanker, L. C. et al. The impact of second to sixth line therapy on survival of relapsed ovarian cancer after primary taxane/platinum-based therapy. *Ann. Oncol.* **23**, 2605–2612 (2012).
5. Bobisse, S. et al. Sensitive and frequent identification of high avidity neo-epitope specific CD8$^+$ T cells in immunotherapy-naive ovarian cancer. *Nat. Commun.* **9**, 1092 (2018).
6. Gronlund, B. et al. Should CA-125 response criteria be preferred to Response Evaluation Criteria in Solid Tumors (RECIST) for prognostication during second-line chemotherapy of ovarian carcinoma? *J. Clin. Oncol.* **22**, 4051–4058 (2004).
7. Jimenez-Sanchez, A. et al. Heterogeneous tumor-immune microenvironments among differentially growing metastases in an ovarian cancer patient. *Cell* **170**, 927–938 (2017).

8. Markman, M. Optimal management of recurrent ovarian cancer. *Int. J. Gynecol. Cancer* **19**, S40–S43 (2009).
9. Goldberg, S. B. et al. Early assessment of lung cancer immunotherapy response via circulating tumor DNA. *Clin. Cancer Res.* **24**, 1872–1880 (2018).
10. Xi, L. et al. Circulating tumor DNA as an early indicator of response to T-cell transfer immunotherapy in metastatic melanoma. *Clin. Cancer Res.* **22**, 5480–5486 (2016).
11. Kandalaft, L. E., Odunsi, K. & Coukos, G. Immunotherapy in ovarian cancer: are we there yet? *J. Clin. Oncol.* **37**, 2460–2471 (2019).
12. Pedersen, M. et al. Adoptive cell therapy with tumor-infiltrating lymphocytes in patients with metastatic ovarian cancer: a pilot study. *Oncoimmunology* **7**, e1502905 (2018).
13. Laport, G. G. et al. Adoptive transfer of costimulated T cells induces lymphocytosis in patients with relapsed/refractory non-Hodgkin lymphoma following $CD34^+$-selected hematopoietic cell transplantation. *Blood* **102**, 2004–2013 (2003).
14. Levine, B. L. et al. Large-scale production of $CD4^+$ T cells from HIV-1-infected donors after CD3/CD28 costimulation. *J. Hematother.* **7**, 437–448 (1998).
15. Jamal-Hanjani, M. et al. Detection of ubiquitous and heterogeneous mutations in cell-free DNA from patients with early-stage non-small-cell lung cancer. *Ann. Oncol.* **27**, 862–867 (2016).

Acknowledgements

We are grateful to the patients for their dedicated collaboration and the healthy donors for their blood donations. We thank the staff of the biobank at the Center for Experimental Therapeutics, University Hospital of Lausanne, for their assistance. We thank J. Michaux, H.S. Pak and P. Hornitschek-Thielan for their excellent technical assistance. We thank D. Monos and his team from the Children's Hospital of Philadelphia for high-resolution human leukocyte antigen typing of patients. We thank A.L. Brennan and the staff of the University of Pennsylvania Clinical Cell and Vaccine Production Facility. We thank S. Schuster and J. Svoboda, who supported the study as independent medical monitors at UPenn. The conduct of the clinical study was supported by National Institutes of Health grants R01FD003520, R21CA156224 and P50CA083638 Specialized Program of Research Excellence in Ovarian Cancer (all to G.C.); 5P30 CA016520-36 Abramson Cancer Center of the University of Pennsylvania Core Support Grant (to B.L.L.); and grants from the Marcus Foundation and the Ovarian Cancer Immunotherapy Initiative (both to G.C.). Tumor sequencing was supported by a grant from the Pennsylvania Department of Health (to G.C.; the department specifically disclaims responsibility for any analyses, interpretations or conclusions). All immune analyses were supported by the Ludwig Institute for Cancer Research and grants from the Ovacure Foundation (to G.C. and A.H.), Biltema Foundation, Paul Matson Foundation and Cancera Foundation (to G.C.). The Vital-IT Center for high-performance computing of the Swiss Institute of Bioinformatics was supported by University of Lausanne/Ecole Polytechnique Fédérale de Lausanne/University of Geneva/University of Bern/Université de Fribourg and the Swiss federal government through the State Secretariat for Education, Research and Innovation.

Author contributions

G.C. designed the clinical study and supervised all activities. J.L.T. and E.Z. provided patient care. S.B. and V.B. conducted experiments, and data analysis and interpretation. A.H. developed and supervised the immune analyses. E.M., R.G., B.J.S., C.I., D.B., M.B.-S., D.G. and R.P. performed sequencing, and data analysis and interpretation. A.S., Z.T. and U.D. performed clinical data analysis and interpretation. F.B., A.M., D.D.L., B.L.L., D.J.P.J., D.A.T., S.A.M. and C.H.J. provided additional support to the experiments and data analysis. L.E.K. was responsible for provision of study resources, materials and patient access. S.B., D.E.S., A.H. and G.C. wrote the paper. All authors reviewed, edited and approved the manuscript.

Competing interests

G.C. has received grants and research support from or has been a coinvestigator in clinical trials for Bristol-Myers Squibb, Celgene, Boehringer Ingelheim, Roche, Tigen Pharma, Iovance and Kite. The Lausanne University Hospital (CHUV) has received honoraria for advisory services G.C. has provided to Roche, Genentech, AstraZeneca AG, Bristol-Myers Squibb SA, F. Hoffmann-La Roche AG, MSD Merck AG and Geneos Therapeutics. G.C. is a coinventor in patents in the domains of tumor-infiltrating lymphocyte (TIL) expansion, T cell engineering, antibodies and tumor vaccines. Patents related to the NeoTIL technology from the Coukos laboratory have been licensed by the Ludwig Institute, also on behalf of the University of Lausanne and the CHUV, to Tigen Pharma. G.C. has previously received royalties from the University of Pennsylvania for CAR-T cell therapy licensed to Novartis and Tmunity Therapeutics. E.Z. has received research support from Merck and Co. and honoraria for advisory services from Celldex and Iovance Biotherapeutics. C.H.J. receives royalties paid from Novartis and Kite to the University of Pennsylvania. C.H.J. is a scientific cofounder and holds equity in Capstan Therapeutics, Dispatch Biotherapeutics and Bluewhale Bio. C.H.J. serves on the board of AC Immune and is a scientific advisor to BluesphereBio, Cabaletta, Carisma, Cartography, Cellares, Cellcarta, Celldex, Danaher, Decheng, ImmuneSensor, Kite, Poseida, Verismo, Viracta and WIRB-Copernicus group. B.L.L. serves on scientific advisory boards for Akron Bio, Avectas, Immuneel, Immusoft, In8bio, Ori Biotech, Oxford Biomedica, Thermo Fisher Scientific, Pharma Services, UTC Therapeutics and Vycellix, and is a cofounder and equity holder of Tmunity Therapeutics (Kite) and Capstan Therapeutics. These relationships are managed in accordance with University of Pennsylvania policy and oversight. The remaining authors declare no competing interests.

Additional information

Extended data is available for this paper at https://doi.org/10.1038/s43018-023-00623-x.

Supplementary information The online version contains supplementary material available at https://doi.org/10.1038/s43018-023-00623-x.

Correspondence and requests for materials should be addressed to George Coukos.

Peer review information *Nature Cancer* thanks Keith Knutson, Masha Kocherginsk and the other, anonymous, reviewer(s) for their contribution to the peer review of this work.

https://doi.org/10.1038/s43018-023-00623-x

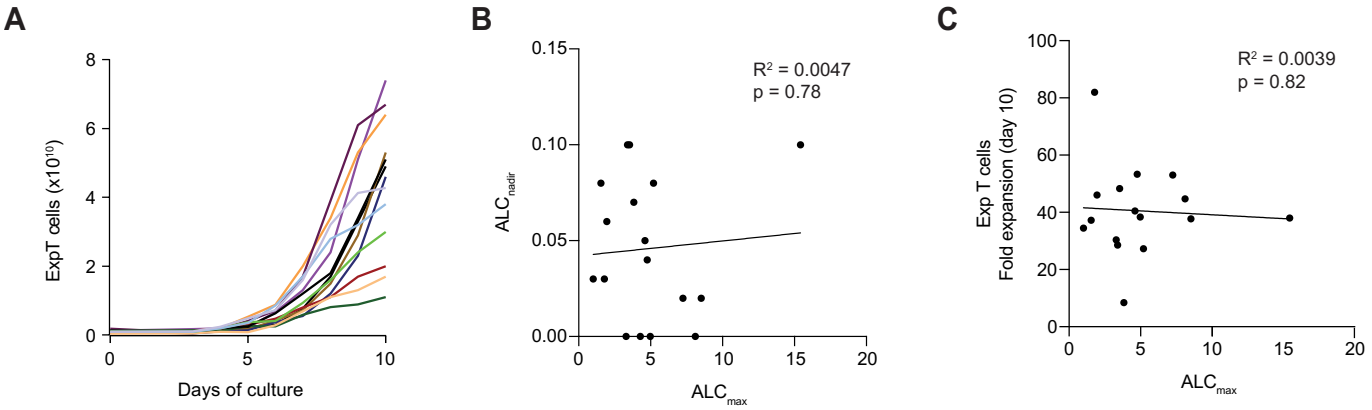

Extended Data Fig. 1 | *In vitro* expansion of cell products and ALC post-ACT. **(A)** T-cell expansion over time during product manufacturing. Exp T cells: expanded T cells (n=13). **(B-C)** Correlation between ALC_{max} observed post-ACT and lowest ALC value (ALC_{nadir}) observed following lymphodepleting chemotherapy and prior to ACT (**B**), and between highest ALC value observed post-ACT (ALC_{max}) and T-cell expansion *in vitro* (**C**). R^2 and p-values were calculated by simple linear regression analysis.

https://doi.org/10.1038/s43018-023-00623-x

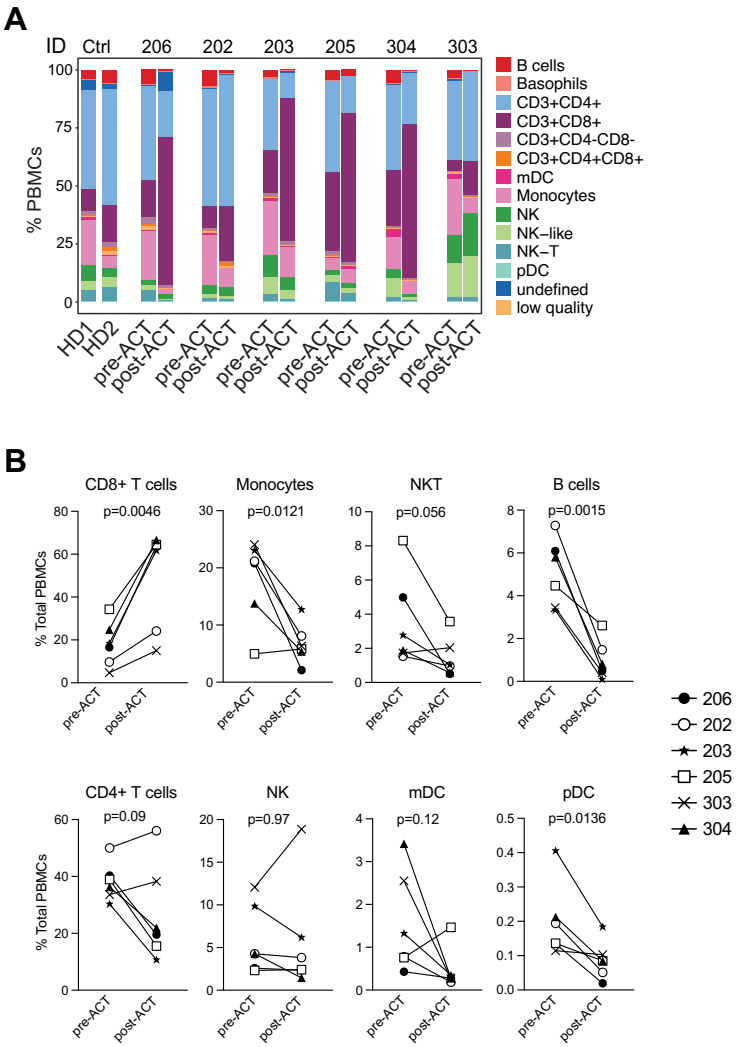

Extended Data Fig. 2 | Immune subsets in blood. (A) Main immune subsets in blood of 6 representative patients pre-lymphodepletion (pre-ACT) and one month post-ACT. HD: healthy donor. **(B)** Frequencies of circulating leukocytes pre-lymphodepletion and one month post-ACT. Paired t-test, two-tailed.

https://doi.org/10.1038/s43018-023-00623-x

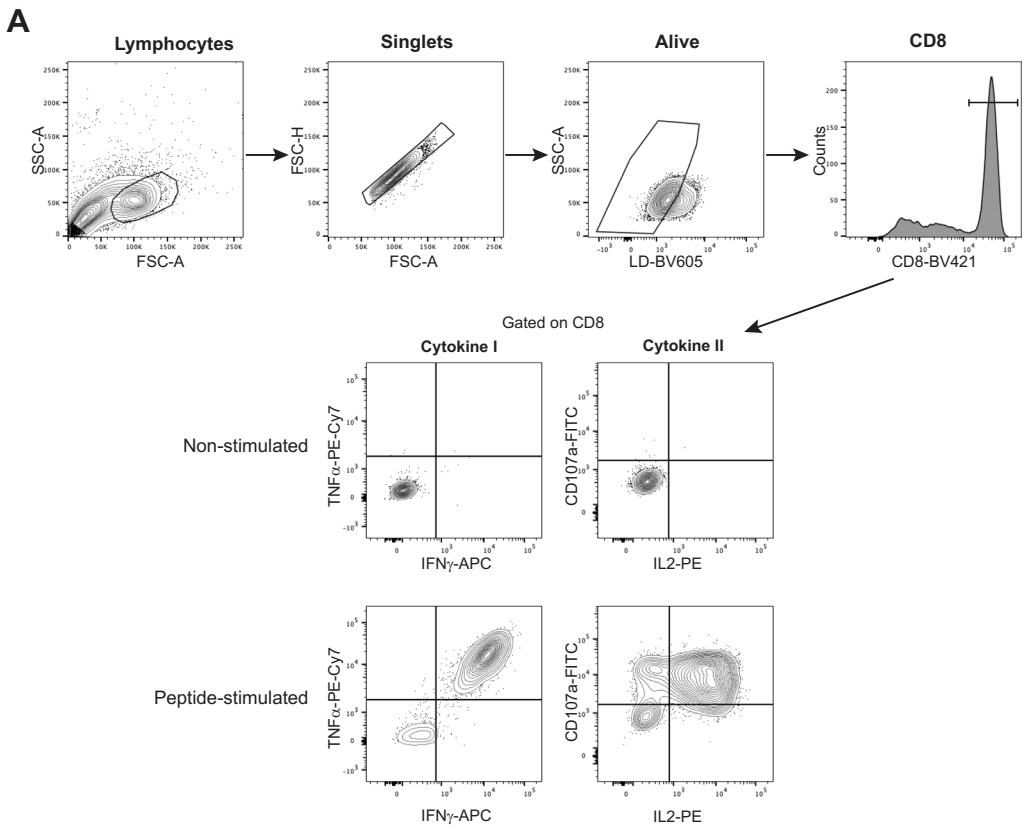

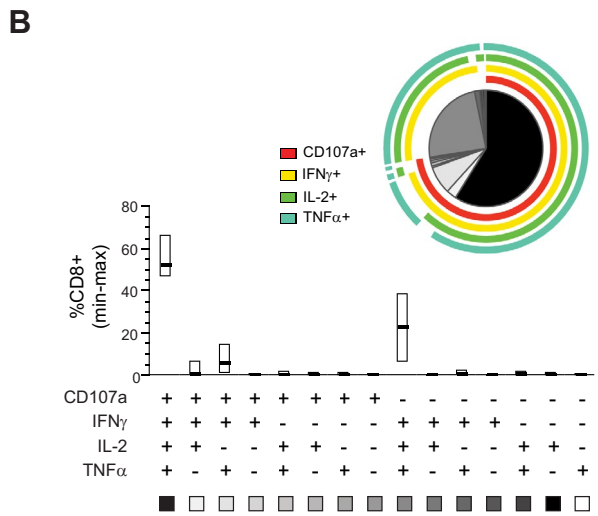

Extended Data Fig. 3 | Intracellular cytokines secretion of neopeptide-specific CD8⁺ T-cells. (**A**) Gating strategy for FACS analysis of ICS assays reported in Fig. 2d. (**B**) Functional profile of neopeptide-specific CD8⁺ T-cells post-ACT (n=3 neopeptides, n=2 patients). The pie chart shows the distribution (mean±SEM) of different functionally distinct subsets of neoantigen-specific CD8⁺ T cells. Individual functions are denoted by arcs. T cells underwent one round of *in vitro* stimulation followed by CD137-sorting and expansion. After 10 days, they were rechallenged with the specific peptide.

https://doi.org/10.1038/s43018-023-00623-x

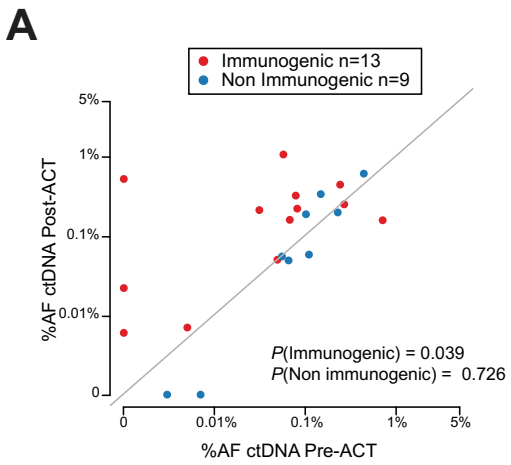

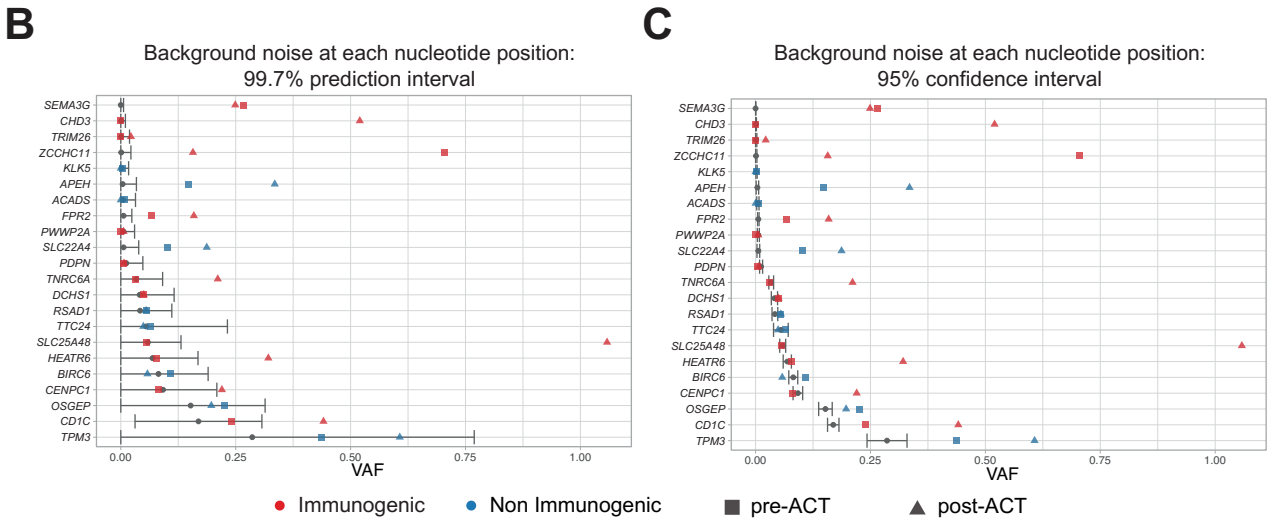

Extended Data Fig. 4 | ctDNA analysis. (A) Allele frequencies (AF, *that is* % of mutated reads over total reads) in ctDNA for the 22 single-nucleotide variants (SNVs) for which were able to build a DNA library. Values observed pre- and post-ACT are shown. Variants are color-coded based on their immunogenicity. Variants showing little or no variation between the two time-points are closer to the diagonal line (dotted grey line). Immunogenic variants showed a significant increase in their AF after ACT (P=0.039). This was not observed among Non-Immunogenic mutations (P=0.726). X and y axes are in logarithmic scales. Comparison of AF in cfDNA for immunogenic and non-immunogenic mutations between pre- and post-ACT was performed using paired samples, one-sided Wilcoxon signed-rank test in the R package (v.3.6.1). **(B)** Estimation of the background noise for each of the SNVs analyzed by ctDNA. Detection of 22 variants in cfDNA with corresponding wild type genes (Supplementary Information). Each gene is reported on one row and it corresponds to annotated immunogenic and non-immunogenic SNVs listed in Extended Data Table 6. Whiskers represent the mean and 99.7% prediction interval (B) or the mean and 95% confidence interval (C). Symbols indicate the AF for each of the 22 mutations detected in cfDNA samples from specific patients, pre-ACT (square) and post-ACT (triangle). We estimated the background distribution through the mean and SD to compute z-score, using a normal approximation for candidate mutations. The ~99.7% prediction interval was standardly defined as a range of 3SD and corrected for aberrant whiskers below zero. P-values were defined as the tail probability and corrected for multiple testing using a Bonferroni correction. Only values with P<0.05 were considered as significantly detected.

https://doi.org/10.1038/s43018-023-00623-x

Extended Data Table 1 | Patients description

UPCC26810 ID	Age	Histology	Stage	Prior Ctx	N Vx pre-ACT	UPCC 19809 RECIST	Days between Vaccination and ACT	N T cell infusions	N Vx post-ACT	UPCC26810 RECIST	CA125 change (day50)
101	60	HGSOC	IIIC	4	5	PD	60	1	1	PD	N (+24%)
102	59	HGSOC	IV	4	5	PR	50	1	5	non-CR/non-PD	N*
103	59	HGSOC	IV	4	5	PD	68	1	4	non-CR/non-PD	Y (-35%)
201	59	Poorly differentiated	IIIC	3	5	SD	53	2	13	SD	Y (-26%)
202	64	HGSOC	IIIC	5	7	SD	375	1	5	SD	Y (-65%)
203	54	HGSOC	IIIC	2	5	PD	32	1	4	PD	Y (-24%)**
204^	75	HGSOC	IIIC	5	8	PD	-	-	-	-	-
205	61	HGSOC	IIIC	5	7	SD	74	1	3	non-CR/non-PD	N (+34%)**
206	48	HGSOC	IV	4	26	SD	53	1	3	non-CR/non-PD	Y (-51%)
301	39	LGSOC	IIIC	3	7	PR	69	2	11	PD	N (+212%)
302	56	HGSOC	IIIC	3	7	SD	117	1	4	non-CR/non-PD	N (+423%)
303	48	HGSOC	IIIC	5	5	PD	313	1	4	non-CR/non-PD	Y (-31%)**
304	69	HGSOC	IIIC	5	16	SD	61	1	5	PD	N*
306	66	Poorly differentiated	IIIC	5	5	SD	151	1	5	SD	Y (-23%)
307	45	HGSOC	IIIC	4	5	SD	284	1	5	non-CR/non-PD	N*
308	54	HGSOC	IV	3	7	PD	292	1	5	PD	N (+7%)
309	51	HGSOC	IIIC	2	5	SD	91	1	5	SD	Y (-10%)
310	65	HGSOC	IV	5	5	PD	54	2	5	SD	N (+28%)

Ctx: Chemotherapy; Vx: Vaccine; Bev: Bevacizumab; Cy: Cyclophosphamide; PD: progressive disease; SD: stable disease; CR: complete responder; PR: partial response; HGSOC: High-Grade Serous Ovarian Cancer; Y: yes; N: no; N*: non contributive CA-125 values (never elevated); **: discordant CA-125 and RECIST evolution; ^patient withdrew from study before T cell infusion due to acute myocardial infarction.

Description of 18 patients enrolled in the study who received the treatment (although 19 patients were initially enrolled, only 18 were treated). Patient identification number, age, tumor histologic type, stage, number of prior chemotherapy lines (Ctx), number of vaccine (Vx) doses received pre-ACT, radiologic response by RECIST v1.1 at end of study of UPCC19809, days between previous treatment and ACT, number of T-cell infusions, number of vaccine doses received post-ACT, radiologic response by RECIST v1.1 and CA-125 response are reported.

 https://doi.org/10.1038/s43018-023-00623-x

Extended Data Table 2 | T-cell products

UPCC26810 ID	Total Cell # started in culture	Total Cell # at end of culture	Total cells fold expansion	$CD3^+$ fraction*	CD3 cell # at end of culture	Final Product Cell #	$CD3^+$ T-cell # in final product*
101	7.40E+08	2.55E+10	34	0.904	2.30E+10	1.50E+10	1.36E+10
102	7.04E+08	5.77E+10	82	0.97	5.60E+10	1.55E+10	1.50E+10
103	9.30E+08	4.28E+10	46	0.967	4.13E+10	1.55E+10	1.50E+10
201	1.00E+09	3.80E+10	38	0.998	3.78E+10	2.74E+10	2.73E+10
202	1.10E+09	3.00E+10	27	0.996	3.00E+10	2.66E+10	2.65E+10
203	4.20E+08	1.70E+10	40	0.953	1.62E+10	1.14E+10	1.09E+10
205	1.30E+09	1.10E+10	8	0.999	1.09E+10	8.94E+09	8.93E+09
206	7.00E+08	2.00E+10	29	0.96	1.94E+10	1.88E+10	1.80E+10
301	1.80E+09	6.70E+10	37	0.906	6.02E+10	2.21E+10	2.00E+10
302	1.20E+09	4.60E+10	38	0.967	4.42E+10	2.07E+10	2.00E+10
303	1.00E+09	5.30E+10	53	0.824	4.36E+10	2.43E+10	2.00E+10
304	1.30E+09	4.90E+10	38	0.937	4.56E+10	2.13E+10	2.00E+10
306	1.20E+09	6.40E+10	53	0.816	5.21E+10	2.45E+10	2.00E+10
307	1.3E+09	7.4E+10	57	0.974	7.25E+10	2.06E+10	2.01E+10
308	1.52E+09	6.80E+10	45	0.944	6.42E+10	2.12E+10	2.00E+10
309	1.50E+09	7.25E+10	48	0.869	6.30E+10	2.30E+10	2.00E+10
310	1.50E+09	4.56E+10	30	0.938	4.28E+10	2.13E+10	2.00E+10

#: number; *at the end of the culture or at day 7

Details of cultured T cells and infused T-cell product per patient.

 https://doi.org/10.1038/s43018-023-00623-x

Extended Data Table 3 | Adverse Events

Individual Events	Grade 1-2 17 patients	Grade 3 17 patients	Grade 4 17 patients
Infection	21	1	
Fatigue	14		
Arthralgia - Myalgia	14		
Abdominal pain	10		
Cutaneous eruption	7		
Constipation	6		
Vomiting	6		
Neuropathy	6		
Diarrhea	5	1	
Nausea	4		
Hypothyroidism	4		
Transaminase elevation	3		
Lymphopenia	3	2	9
Alopecia	3		
CNS	3	2	
Proteinuria	2		1
Anemia	2		
Neutropenia	2	5	4
Leucopenia	2	6	3
Hypertension	2		
Hyperthermia	1		
Infusion reaction	1		
Dyspnea	1		
Bowel obstruction		1	
Hypophosphatemia		1	
Hypokalemia		1	
Febrile neutropenia		1	
Thrombocytopenia			
Dehydration		3	
Acute myocardial infarction		1	
Seizure		1	
TOTAL N. EVENTS	122	26	17

Description of Adverse Events.

 https://doi.org/10.1038/s43018-023-00623-x

Extended Data Table 4 | Neopeptide recognition landscape

UPCC26810 ID	# Non-synonymous Mutations	HLA-A	HLA-B	HLA-C	Immunogenic neoantigens pre-ACT	Immunogenic neoantigens post-ACT
101	47	23:01 29:01	39:06 44:03	04:01 07:02	-	-
102	10	23:01 23:01	14:02 50:01	06:02 08:02	$HS6ST1_{S405I}$	$HS6ST1_{S405I}$
201	95	01:01 25:01	07:02 08:01	07:01 07:02	-	$PWWP2A_{F753Y}$
202	36	02:01 03:01	35:01 40:01	03:04 04:01	-	$HS6ST1_{S405I}$
203	117	24:02 69:01	15:01 51:01	03:03 16:02	$SEMA3G_{P412A}$, $CD1C_{F34L}$	$FPR2_{D71V}$, $SLC25A48_{V200M}$, $CD1C_{F34L}$
205	90	02:01 31:01	15:01 35:02	03:03 04:01	$TRIM26_{G497W}$, $CHD3_{L542V}$, $DCHS1_{P141L}$, $EBF4_{I510S}$	$TRIM26_{G497W}$, $CHD3_{L542V}$, $HEATR6_{S515N}$
206	85	32:01 68:01	15:01 44:02	02:02 07:04	-	$CENPC1_{R738H}$
301	38	01:01 24:02	15:17 51:01	02:02 07:01	-	-
303	105	11:01 02:14	07:02 27:05	02:02 07:02	$ZCCHC11_{P1265H}$, $OR2T3_{C132Y}$, $TNRC6A_{P312Q}$	$ZCCHC11_{P1265H}$, $OR2T3_{C132Y}$, $TNRC6A_{P312Q}$
304	129	02:01 33:01	14:02 14:02	08:02 08:02	$KIR2DS4_{I7S}$, $PDPN_{G222C}$	$KIR2DS4_{I7S}$, $PDPN_{G222C}$
306	34	24:02 26:01	07:02 39:06	07:02 07:02	-	-

#: number

Description of the neopeptide recognition landscape. Individual tumor mutational burden (non-synonymous mutations), haplotypes and predicted peptides found immunogenic at two time points (pre- and post-ACT) are reported.

 https://doi.org/10.1038/s43018-023-00623-x

Extended Data Table 5 | Neopeptide characteristics

UPCC26810 ID	Gene	Mutation	HLA restriction	Sequence
102	HS6ST1	S405I	A23:01	DYM**I**HIIEKW
201	PWWP2A	F753Y	A25:01	EVRALLTQ**Y**
202	HS6ST1	S405I	B40:01	TEDYM**I**HII
203	SEMA3G	P412A	B15:01	FARAH**A**LMF
203	FPR2	D71V	A24:02	**V**FSFTATLPF
203	SLC25A48	V200M	A24:02	PY**M**FLSEWI
203	CD1C	F34L	A69:01	HVIQI**L**SFV
205	TRIM26	G497W	B15:01	LDYE**W**GTVTF
205	CHD3	L542V	A02:01	HIHC**V**NPPL
205	EBF4	I510S	B15:01	A**S**MPSSPPL
205	DCHS1	P141L	C03:03	VADINDHA**L**
205	HEATR6	S515N	A02:01	VMIAC**N**IREL
206	CENPC1	R738H	A68:01	NTPNV**H**RTKR
303	ZCCHC11	P1265H	B27:05	GRKLFGT**H**F
303	OR2T3	C132Y	C07:02	**Y**RPLHYPLLM
303	TNRC6A	P59Q	B27:05	G**Q**WGFSHGA
304	KIR2DS4	I7S	A02:01	I**S**MACVGFFL
304	PDPN	G222C	A02:01	FI**C**AIIVVV

List of 18 immunogenic peptides classified by patient and described by coding gene, mutation, HLA restriction and full sequence.

 https://doi.org/10.1038/s43018-023-00623-x

Extended Data Table 6 | ctDNA analysis

UPCC26810 ID	Chromosome	Position	AAchange	Immunogenicity	Call	VAF GATK
206	chr8	103573006	S216N	SNP	SNP	NON_VARIANT
202	chr1	156814027	P928L	SNP	SNP	NON_VARIANT
202	chr14	94776221	S246A	SNP	SNP	NON_VARIANT
102	chr3	24006477	L386M	SNP	SNP	NON_VARIANT
102	chr6	28264692	Q248E	SNP	SNP	NON_VARIANT
201	chr2	241465261	T175I	SNP	SNP	NON_VARIANT
201	chr8	144775871	L93I	SNP	SNP	NON_VARIANT
203	chr7	100550138	T240M	SNP	SNP	NON_VARIANT
203	chr10	50034833	G2034S	SNP	SNP	NON_VARIANT
205	chr9	138440527	L98S	SNP	SNP	NON_VARIANT
205	chr13	46629944	I347T	SNP	SNP	NON_VARIANT
304	chr1	247752367	R236G	SNP	SNP	NON_VARIANT
304	chr3	142281612	M211T	SNP	SNP	NON_VARIANT
303	chr4	5624670	T699A	SNP	SNP	NON_VARIANT
303	chr19	57648277	L69M	SNP	SNP	NON_VARIANT
303	chr3	49719351	W518C	Non Immuno	SM	0.586
303	chr14	20922752	T31A	Non Immuno	SM	0.374
205	chr2	32768522	G4169D	Non Immuno	SM	0.339
304	chr17	48561824	Q377K	Non Immuno	SM	0.325
203	chr5	131647878	W140R	Non Immuno	SM	0.235
203	chr1	154131496	N231K	Non Immuno	SM	0.215
205	chr1	156553634	D400N	Non Immuno	SM	0.163
304	chr19	51453312	G45V	Non Immuno	SM	0.143
201	chr12	121176159	R234Q	Non Immuno	SM	0.111
205	chr17	58137330	S54N	Immuno	SM	0.769
205	chr11	6662423	P141L	Immuno	SM	0.552
205	chr17	7798412	L542V	Immuno	SM	0.458
303	chr16	24800898	P59Q	Immuno	SM	0.339
206	chr4	68359679	R738H	Immuno	SM	0.324
303	chr1	52911487	P1265H	Immuno	SM	0.289
203	chr1	158260962	F34L	Immuno	SM	0.261
203	chr5	135207326	V200M	Immuno	SM	0.242
304	chr1	13940860	G222C	Immuno	SM	0.217
203	chr19	52272123	D71V	Immuno	SM	0.181
205	chr6	30153784	G497W	Immuno	SM	0.163
201	chr5	159519399	F753Y	Immuno	SM	0.155
203	chr3	52474024	P412A	Immuno	SM	0.151

Details of single nucleotide variants (SNVs) successfully investigated by ctDNA analysis, classified by patient, chromosome, position, amino acid change, immunogenicity (single nucleotide polymorphism (SNP), Non immuno: non-immunogenic mutation, Immuno: immunogenic mutations) and call (SNP, or somatic mutations (SM)). Notably, all SM were called by all three GATK HaplotypeCaller (GATK), Mutect_v1 (MTv1) and Varscan2 (VS2) algorithms. VAF: variant allele frequency, as predicted by GATK.

nature portfolio

Corresponding author(s): George Coukos

Last updated by author(s): 2022/06/16

Reporting Summary

Nature Portfolio wishes to improve the reproducibility of the work that we publish. This form provides structure for consistency and transparency in reporting. For further information on Nature Portfolio policies, see our Editorial Policies and the Editorial Policy Checklist.

Statistics

For all statistical analyses, confirm that the following items are present in the figure legend, table legend, main text, or Methods section.

n/a	Confirmed
☐	☒ The exact sample size (*n*) for each experimental group/condition, given as a discrete number and unit of measurement
☐	☒ A statement on whether measurements were taken from distinct samples or whether the same sample was measured repeatedly
☐	☒ The statistical test(s) used AND whether they are one- or two-sided *Only common tests should be described solely by name; describe more complex techniques in the Methods section.*
☒	☐ A description of all covariates tested
☐	☒ A description of any assumptions or corrections, such as tests of normality and adjustment for multiple comparisons
☐	☒ A full description of the statistical parameters including central tendency (e.g. means) or other basic estimates (e.g. regression coefficient) AND variation (e.g. standard deviation) or associated estimates of uncertainty (e.g. confidence intervals)
☐	☒ For null hypothesis testing, the test statistic (e.g. *F*, *t*, *r*) with confidence intervals, effect sizes, degrees of freedom and *P* value noted *Give P values as exact values whenever suitable.*
☒	☐ For Bayesian analysis, information on the choice of priors and Markov chain Monte Carlo settings
☒	☐ For hierarchical and complex designs, identification of the appropriate level for tests and full reporting of outcomes
☒	☐ Estimates of effect sizes (e.g. Cohen's *d*, Pearson's *r*), indicating how they were calculated

Our web collection on statistics for biologists contains articles on many of the points above.

Software and code

Policy information about availability of computer code

Data collection	Demographic and disease characteristics of all eligible patients were collected for analysis including age, initial disease stage and histology, and number of prior treatment lines. The number of OCDC administrations before ACT and co-medications within the NCT01132014/ UPCC19809 study, as well as the number of post-ACT OCDC administrations was recorded. The best radiological response per RECIST, CA-125 values longitudinally prior and after ACT and time to death from enrolment into NCT01312376/UPCC26810 were collected. WES was performed using a HiSeq2500 Illumina platform. ELIspot plates were counted with a Bioreader-6000-E (BioSys). Flow cytometry data were collected with a BD Fortessa or BD FACS Melody (BD Biosciences). For cfDNA sequencing, a Ion PGM System and a Ion S5™ System were used. FASQ files were generated using the Torrent suite software (v.5.2.2).
Data analysis	Neoepitope binding prediction was performed using netMHC v3.4. For cfDNA analyses Novoalign (V3.02.07), bam-readcount (v0.8.0) and IGV software (v2.3) were used. Flow Cytometry data were analysed with FlowJo 10.8.1, SPICE 6.1, RStudio v3.5.1, FlowSOM and openCyto. For graphical analysis and statistical tests GraphPad Prism v9, SAS v9.4 and R v4.0.3 were used.

For manuscripts utilizing custom algorithms or software that are central to the research but not yet described in published literature, software must be made available to editors and reviewers. We strongly encourage code deposition in a community repository (e.g. GitHub). See the Nature Portfolio guidelines for submitting code & software for further information.

Data

Policy information about availability of data

All manuscripts must include a data availability statement. This statement should provide the following information, where applicable:

- Accession codes, unique identifiers, or web links for publicly available datasets
- A description of any restrictions on data availability
- For clinical datasets or third party data, please ensure that the statement adheres to our policy

Exome data have been deposited in the European Genome-phenome Archive (EGA) database under the accession code EGAS00001002803. Individual patients are identified by a CTE code matching their UPCC26810 numbers (reported in the text). Matched IDs are the following: lOl=CTE-0004; 102=CTE-0005; 201=CTE-0007; 202=CTE-0003; 203=CTE-0008; 205=CTE-0010; 206=CTE-0001; 301=CTE-0017; 303=CTE-0015; 304=CTE-0012; 306=CTE-0018.
cfDNA amplicon data were highly redundant and would unnecessarily occupy space in the public repository, still they are available from the authors upon request.
The authors declare that additional data supporting the findings of this study are available within the article and its Extended Data.

Human research participants

Policy information about studies involving human research participants and Sex and Gender in Research.

Reporting on sex and gender	Gender specification is unnecessary in this study and the terms sex and gender have never been mentioned in the text. Participants are all subjects affected by a type of cancer originated in the female reproductive apparatus.
Population characteristics	Eligible patients had a diagnosis of epithelial ovarian, fallopian tube or primary peritoneal adenocarcinoma, and exhibited persistent or progressive disease by RECIST to intervening therapy or in prior protocol NCT01132014/UPCC19809 after at least five vaccine administrations. All patients were ≥18 years old, and required to have an Eastern Cooperative Oncology Group performance (ECOG) status 0 or 1 with a life expectancy of >4 months. All patients had normal organ and bone marrow function defined by an absolute neutrophil count greater than 1,000/microL, platelet count greater than 100,000/microL, hematocrit greater than 30%, aspartate transaminase (AST) and alanine transaminase (ALT) less than 2.5 times the institutional upper limit of normal, bilirubin less than 2.0 mg/dL unless secondary to bile duct blockage by tumor, and creatinine less than 1.8 mg/dL. Non-eligibility criteria included history or symptoms suggestive of partial or complete bowel obstruction, more than two-week corticosteroid treatment or other immune-suppressive treatment, acute infections and acquired clinically significant concomitant conditions contraindicating study therapy or interfering with result interpretation. Presence of serum anti-Yo antibodies on screening, irrespective of clinical relevance, was an exclusion criterion.
Recruitment	All participants signed the informed consent form. Patients were eligible for UPCC26810 provided peripheral blood T cells had been collected through apheresis after vaccination on the UPCC19809 study and they had at least two more vaccine doses available.
Ethics oversight	For patients' samples: regulatory committee of UPenn; For healthy donors: collection following the legal Swiss guidelines under the project P_123 with informed consent of the donors and with Ethics Approval from the Canton of Vaud (Lausanne).

Note that full information on the approval of the study protocol must also be provided in the manuscript.

Field-specific reporting

Please select the one below that is the best fit for your research. If you are not sure, read the appropriate sections before making your selection.

☒ Life sciences ☐ Behavioural & social sciences ☐ Ecological, evolutionary & environmental sciences

For a reference copy of the document with all sections, see nature.com/documents/nr-reporting-summary-flat.pdf

Life sciences study design

All studies must disclose on these points even when the disclosure is negative.

Sample size	Eligible patients enrolled in the pilot study were n=18. One patient withdrew form study before treatment. No statistical methods were used to pre-determine sample sizes but our sample sizes are similar to those reported in previous publications (doi: 10.1126/scitranslmed.aao5931). Exome-sequencing was performed on n=11 representative patients. For in vitro studies, the number of samples and/or technical replicates were chosen according to the complexity of the assay and the expected biological variability. All private mutations matching peptides targeted by T cells (i.e. immunogenic mutations) were considered for cfDNA analysis. Only a subset was successfully processed and all data are included in the analysis.
Data exclusions	No data were excluded from analyses.
Replication	Replication of in vitro studies using patient PBMCs and sera were constrained by sample availability. All neoepitope-specific T cell responses

Replication	were successfully replicated at least twice. To validate immunogenic peptide(s), replicate independent experiments were performed after one round of IVS with peptide pool(s) and/or single immunogenic peptides (n=2). Alternatively, when samples were not available, a second round of stimulation (IVS2) was performed to further validate T-cell responses.
Randomization	We did not randomize patients as the primary objectives were safety and feasibility.
Blinding	We did not use blinding as the primary objective was safety and feasibility.

Reporting for specific materials, systems and methods

We require information from authors about some types of materials, experimental systems and methods used in many studies. Here, indicate whether each material, system or method listed is relevant to your study. If you are not sure if a list item applies to your research, read the appropriate section before selecting a response.

Materials & experimental systems

n/a	Involved in the study
☐	☒ Antibodies
☒	☐ Eukaryotic cell lines
☒	☐ Palaeontology and archaeology
☒	☐ Animals and other organisms
☐	☒ Clinical data
☒	☐ Dual use research of concern

Methods

n/a	Involved in the study
☒	☐ ChIP-seq
☐	☒ Flow cytometry
☒	☐ MRI-based neuroimaging

Antibodies

Antibodies used	Antibodies were titrated for optimal staining. Aqua live Dye BVSlO (L34966, Thermo Fisher Scientific) or Zombie UV (77474, Biolegend) were used to assess viability. The immune profiling antibody panel included the following fluorophore conjugated antibodies: mouse anti-human CD3-APC (clone UCHTl, cat. IM2467, Beckman Coulter, 2uL/100uL staining mix; final dilution 1:50); mouse anti-human CD4-PECy7 (clone SFCl12T4Dll, cat. 737660, Beckman Coulter, 0.4uL/100uL staining mix, final dilution 1:250); mouse anti-human CDS-Pacific Blue (clon RPA-T8, cat.558207, BD Biosciences, 7uL, final dilution 1:15); mouse anti-human CD14-APC H7 (clone Mϕ P9, cat.641394, BD Biosciences, 8uL final dilution 1:12.5); mouse anti-human CD16-FITC (clone 3G8, cat.555406, BD Biosciences, 5 ul final dilution 1:20); CD56-PE (clone N901, cta.A07788, Beckman Coulter, 10uL, final dilution 1:10); mouse anti-human CD11c-AF700 (clone B-ly6, cat.561352, BD Biosciences, 2uL, final dilution 1:50); mouse anti-human CD19-BV711 (clone SJ25Cl, cat.563036, BD Biosciences, 3uL, final dilution 1:33); mouse anti-human CD123-PerCP CyS.5 (clone 6H6, cat.45-1239-42, Thermo Fisher Scientific, 2uL, final dilution 1:50); mouse anti-human HLA-DR-ECD (clone B8.12.2, cat.lM3636, Beckman Coulter, 2uL final dilution 1:50). For sorting of neo-epitope specific T cells the following antibodies were used: mouse anti-human CD3-APC Fire 750 (clone SK7, cat. 344840, Biolegend, 2uL/100uL staining mix, final dilution 1:50); mouse anti-human CDS-Pacific Blue (clone RPA-T8, cat. 558207, BD Biosciences, 3uL/100uL staining mix, final dilution 1:33); and mouse anti-human 137-PE (clone 4B4-1, cat. 130-119-885, Miltenyi Biotec, 2uL/100uL staining mix, final dilution 1:50). For intracellular cytokine staining the following fluorophore conjugated antibodies were used: mouse anti-human CD107a-FITC (clone H4A3, cat. 555800, BD Pharmingen; 3uL in 100uL of cell suspension in medium); mouse anti-human CD3-APC Fire 750 (clone SK7, cat. 344840, Biolegend, luL/lO0uL staining mix, final dilution 1:100); mouse anti-human CDS-Pacific Blue (clone RPA-T8, cat. 558207, BD Biosciences, 3uL/100uL staining mix, final dilution 1:33); mouse anti-human IL-2-PE(clone 5344.111, cat. 340450, BD Biosciences, 20uL/100uL staining mix, final dilution 1:5); mouse anti-human TNFα PE Cy7 (clone Mabll, cat. 557647, BD Biosciences, 5uL/100uL staining mix, final dilution 1:20); and mouse anti-human IFNγ APC (clone B27, cat. 554702, BD Biosciences, 0.3uL/100uL, final dilution 1:333).
Validation	Antibodies' concentrations validation was empirically determined in the lab, as per manufacturers' instructions. All primary antibodies were validated and titrated with human PBMCs or additional irrelevant cells that were either activated or resting depending on each antibody using Fortessa and Melody BD Biosciences flow cytometers.

Clinical data

Policy information about clinical studies

All manuscripts should comply with the ICMJE guidelines for publication of clinical research and a completed CONSORT checklist must be included with all submissions.

Clinical trial registration	NCT01312376/UPCC26810
Study protocol	The full study protocol is publicly available and confidentially provided as supporting material.
Data collection	The study was conducted in the Service of Gynecologic Oncology at the University of Pennsylvania Medical Center, with patient enrollment and patient sample and data collection from 2010 to 2016.
Outcomes	The primary objective was to determine the feasibility and safety of vaccine-primed, ex vivo CD3/CD28-costimulated autologous peripheral blood T-cells, in combination with lymphodepletion and an immunomodulation regimen of Bevacizumab followed by autologous vaccination. Feasibility was assessed based on the number of patients who have successfully received the combination treatment. Safety was assessed based on the occurrence of treatment-limiting toxicities (TLTs). If a TLT was observed in more than

33% of patients, then the therapy was considered too toxic (>33% of patients with toxicity as not acceptable). Additional objectives included immune function, anti-tumor immune response, tumor burden, immune related (ir)-progression-free survival, overall survival and time to progression.

Flow Cytometry

Plots

Confirm that:

☒ The axis labels state the marker and fluorochrome used (e.g. CD4-FITC).

☒ The axis scales are clearly visible. Include numbers along axes only for bottom left plot of group (a 'group' is an analysis of identical markers).

☒ All plots are contour plots with outliers or pseudocolor plots.

☒ A numerical value for number of cells or percentage (with statistics) is provided.

Methodology

Sample preparation	For ex vivo PBMC phenotyping, cells were thawed, washed twice in complete cell culture medium (RPMI, 10% FBS), washed once in PBS and resuspended in PBS containing LIVE/DEAD dye and the antibody cocktail for cell surface staining (either panel 1 or panel 2 at the Antibodies section of the present document). Cells were incubated at 4°C for 20-30 minutes and washed twice before acquisition. For intracellular cytokine staining, T cells stimulated in vitro for 12 days were re-stimulated with peptide-pulsed autologous CD4+ blasts (ratio 1:1) in the presence of GolgiPlug and CD107a antibody. After 16-18 hours, cells were harvested, washed once in PBS and resuspended in FACS buffer containing cell surface staining antibodies (CD3, CD4, CD8). Cells were incubated at 4°C for 20 minutes, washed in PBS, then resuspended in Cytofix/Cytoperm (BD) for permeabilisation and incubated at 4°C for 20 minutes. After one washing step in Perm Wash (buffer (BD), cells were resuspended in Perm Wash buffer containing cytokine-specific antibodies and the viability dye. After one final washing step in Perm Wash, cells were resuspended in FACS buffer and acquired. Cells were not fixed prior to acquisition.
Instrument	BD Fortezza and BD FACS Melody
Software	FlowJo 10.8.1, SPICE 6.1, RStudio v3.5.1, FlowSOM and openCyto.
Cell population abundance	Immune profiling (i.e. FACS staining) was performed by using 1.5x10E6 total PBMCs per sample. T cell samples enriched in neo-epitope-specific T cells were co-cultured with CD4 blasts starting from 2x10E5 cells and up to 10E6 cells. All cells were collected and stained for intracellular cytokines.
Gating strategy	For the immune phenotype of PBMCs, gating and analysis strategy are stated in the Methods section. For intracellular cytokine staining: starting cell population was gated on a linear SSC-A/FSC-A plot. Single cells were discriminated on a linear FSC-H or FSC-W/FSC-A plot. Live cells were determined by exclusion from positive Live/Dead stained cells. Positive/Negative populations for CD3, CD4 and CD8 surface markers were determined with unstained negative controls. All other positive/negative populations were determined with unstimulated T cells (i.e. matched T cells incubated in teh same conditions but in the absence of CD4 blast cells).

☒ Tick this box to confirm that a figure exemplifying the gating strategy is provided in the Supplementary Information.